



Fast Directional Handoff and lightweight retransmission protocol for enhancing multimedia quality in indoor WLANs



Sangyup Han^a, Myungchul Kim^{a,*}, Ben Lee^b, Sungwon Kang^a

^a The Department of Computer Science, Korea Advanced Institute of Science and Technology, Republic of Korea

^b The School of Electrical Engineering and Computer Science, Oregon State University, Corvallis, OR 97330, USA

ARTICLE INFO

Article history:

Received 24 February 2014

Received in revised form 1 November 2014

Accepted 31 December 2014

Available online 9 January 2015

Keywords:

IEEE 802.11

Fast Directional Handoff

Geomagnetic sensor

Digital compass

Lightweight retransmission protocol

ABSTRACT

More and more mobile devices such as smartphones are being used with IEEE 802.11 wireless LANs (WLANs or Wi-Fi). However, mobile users are still experiencing poor service quality on the move due to the large handoff delay and packet loss problem. In order to reduce the delay, a new handoff scheme using the geomagnetic sensor embedded in mobile devices is proposed in this paper. The proposed scheme predicts the movement direction of a Mobile Station (MS) from the currently associated Access Point (AP) and performs active scanning with a reduced number of channels. In terms of the packet loss, a lightweight retransmission protocol is also proposed to minimize lost packets on Wi-Fi without producing a lot of acknowledgement packets. The proposed approaches are implemented on Android smartphones, and their performance is evaluated in a real indoor WLAN environment. The evaluation results demonstrate that the proposed schemes maintain seamless quality for real-time video even in an environment with frequent handoffs. Note that the proposed schemes are a client-only solution and do not require modification of the existing APs, which renders them very practical.

© 2015 Elsevier B.V. All rights reserved.

1. Introduction

With the popularity of smartphones and pad/tablet devices, more and more mobile users are relying on IEEE 802.11 wireless LANs (WLANs or Wi-Fi) for multimedia services due to their high data rate and low cost. However, because WLANs do not support fast handoff from one Access Point (AP) to another, users on the move may experience significant delays or even lose connectivity during real-time multimedia services, such as Voice over IP (VoIP) and video conferencing.

Fast handoff in WLANs is achieved through minimizing the time required to scan for available APs. This requires knowledge of the location and/or movement direction of

the Mobile Stations (MSs) in order to improve the accuracy of the next AP prediction for association. The easiest method of determining the location is to use a Global Positioning System (GPS) [2]. However, the power requirements of a GPS and the delay incurred in retrieving the location information are very high, and GPSs cannot be used in indoor environments. Another method of determining locations is using a Wi-Fi Positioning System (WPS) [3]. However, a WPS may not be practical because its implementation and deployment require excessive time and manpower. In the absence of GPS or WPS, most prior work on reducing the scanning delay involves limiting the number of channels to scan based on the history of past scans [4,5], mobility patterns [6], and periodically scanning neighboring channels [7,8]. However, these schemes either cause handoffs to incorrect APs [4–6], require modification of the existing APs [6,7], or do not reduce the scanning delay, as in the case of IEEE 802.11n/ac [4,5].

* Corresponding author.

E-mail addresses: ilu8318@kaist.ac.kr (S. Han), mck@kaist.ac.kr (M. Kim), benl@eecs.orst.edu (B. Lee), sungwon.kang@kaist.ac.kr (S. Kang).

In addition, none of the previous works consider the quality of real-time multimedia in terms of Quality of Experience (QoE). Because the degradation of the multimedia quality on the move becomes another cause of restricting user mobility, it is as important as reducing handoff delay and must be considered in conjunction with the handoff delay.

Therefore, this paper proposes the *Directional Handoff (DH) scheme* and the *Lightweight Retransmission Protocol (LRP)* in order to provide both a reduced handoff delay and a constant quality level of multimedia. The DH scheme predicts the direction of an MS using a geomagnetic sensor and reduces the handoff delay by limiting the number of candidate APs for scanning to only one or two APs. Also, the LRP minimizes the number of lost video packets through retransmission and effectively ensures the timely play-out of video packets using a play-out timer. Therefore, in addition to providing a discussion of the DH scheme, the specific contributions of this paper are as follows:

1. The DH scheme with the LRP reduces the handoff delay and provides a consistent quality level in order to support real-time multimedia services.
2. This is the first paper that investigates the video quality in a real environment where frequent handoffs occur.
3. The DH scheme with the LRP is fully automated without need for preconfiguration.
4. The DH scheme with the LRP can be used regardless of the IEEE 802.11b/g/n/ac standards and the number of channels supported by the standards.
5. Commercial smartphones are used to implement and demonstrate the performance of the methods.

The experimental study presented in this paper uses three testbeds to demonstrate that the proposed DH scheme achieves an approximately 50% lower handoff delay than the conventional handoff and selective scanning scheme [4]. In addition, the DH scheme with the LRP maintains the visual quality of real-time video even in an environment with frequent handoffs; thus, mobile users can use real-time multimedia services without noticing the existence of handoffs.

This paper is organized as follows. Section 2 discusses the background and previous studies on fast handoff in WLANs. Section 3 presents the DH scheme; Section 4 describes the implementation of the DH scheme on commercial smartphones and discusses the experimental setup and results. Section 5 proposes the LRP for mobile users and discusses its experimental results. Finally, Section 6 concludes the paper and discusses future work.

2. Background and related work

2.1. Background of fast handoff and video delivery

A handoff in IEEE 802.11 WLANs consists of three steps: scanning, authentication, and re-association [9]. *Scanning* is the process of finding new APs for connection. The next AP to handoff to is chosen from the scanning result by considering various factors, such as the Received Signal

Strength Indicator (RSSI). After determining the target AP, the *authentication* process sends information of the MS to the new AP. After authentication, the *re-association* process requests reconnection to the new AP. The handoff process is complete when the MS is allowed to reconnect. Therefore, the handoff delay is defined as the sum of the time required in each step and is given as follows:

$$T_{Handoff} = T_{Scanning} + T_{Authen.} + T_{Reassoc.} \quad (1)$$

The time required for an MS to switch to another channel is negligible and thus is not included in Eq. (1). The overall handoff delay is typically in the range of 200–400 ms, and the scanning step represents approximately 90% of the delay [9]. The authentication and re-association steps require up to 10 ms each and have a minimal impact on the overall delay.

The scanning process dominates the handoff delay as a result of the scanning method used and the number of channels scanned. There are two scanning methods: passive scanning and active scanning. *Passive scanning* locates APs by listening to the beacon frames that are periodically transmitted by APs; these are typically transmitted every 100 ms. As a result, an MS must wait as long as 100 ms for a single channel in order to receive the beacon frames. Therefore, the time required for passive scanning (T_{PS}) with N channels is defined as follows:

$$T_{PS} = N \times BeaconInterval \quad (2)$$

There are at least 11 channels in IEEE 802.11b/g [10], and thus passive scanning requires more than 1 s. Because the International Telecommunication Union (ITU) recommends that the handoff delay for real-time multimedia applications should not exceed 150 ms [11], passive scanning is unsuitable and causes severe disruptions for real-time multimedia services.

In *active scanning*, an MS sends probe request frames to APs through either broadcasting or unicasting. An MS sends the probe request frames and then it waits for the corresponding response frames for each channel. Therefore, the time taken for active scanning (T_{AS}) is defined as follows:

$$N \times T_{MinChannel} \leq T_{AS} \leq N \times T_{MaxChannel}, \quad (3)$$

where $T_{MinChannel}$ and $T_{MaxChannel}$ represent *MinChannelTime* and *MaxChannelTime*, respectively. First, an MS sends probe request frames and waits for *MinChannelTime*. If it does not receive any probe response frames within this time, it switches to the next channel. Otherwise, it receives more probe response frames until *MaxChannelTime* and then switches to the next channel.

A prior study demonstrated that 6.5 ms and 11 ms are appropriate choices for the *MinChannelTime* and *MaxChannelTime*, respectively [9]. Therefore, the active scanning delay in IEEE 802.11b/g can be up to 121 ms, and the handoff delay can be up to 141 ms.

In case of the IEEE 802.11n/ac protocol using the 5 GHz band, there are at least 19 channels [12], and both the passive and active scanning methods are used separately based on the channel number, as shown in Fig. 1. When an MS scans the Dynamic Frequency Selection (DFS) channels (channel numbers 52–140), it must use the passive

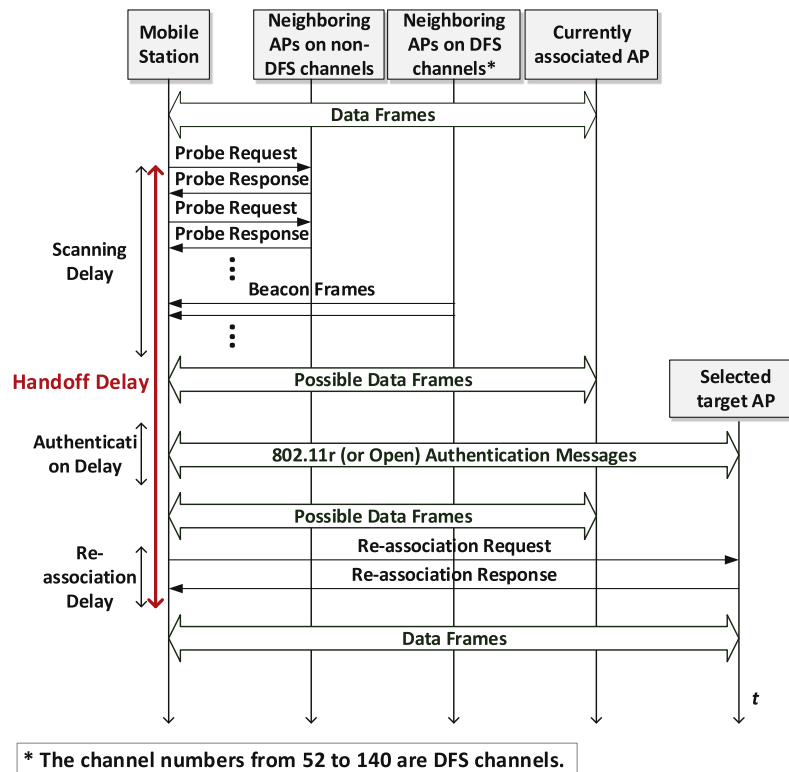


Fig. 1. A typical handoff procedure in the 5 GHz band of the IEEE 802.11n/ac protocol.

scanning in order to avoid interfering with possible radars that already use those channels [13]. Because there are at least 11 DFS channels in South Korea and United States, the time required for scanning increases further [12]. Therefore, the conventional handoff that scans all channels is not suitable for real-time multimedia services.

In addition, the packet loss problem that affects the visual quality of real-time video is as important as the handoff delay. If the visual quality degrades when the MS is moving, the mobility is restricted as mobile users would be reluctant to move during video conferencing. Although handoff delay can be reduced using a fast handoff, the quality of real-time video cannot be guaranteed due to packet losses. The current video codecs, e.g. MPEG-2 and H.264/AVC, are based on inter-prediction where a video frame is decoded using previous or reference frames. Therefore, even if one packet is lost in a video frame, the quality of several subsequent frames may be affected.

There are many causes of packet loss including handoff, interference, noise, the hidden node problem, and low signal strength [14]. The video quality degradation due to packet losses is particularly severe on the edge of an AP's coverage area where handoffs occur due to a low signal strength. Moreover, the packet loss problem has recently become more severe due to the rapid increase in the number of MSs and densely deployed APs. Therefore, it is important to consider the packet losses that occur not only at the time of handoffs but also around the time of handoffs.

2.2. Related work on fast handoff

Shin et al. proposed the *selective scanning and caching* [4]. The *selective scanning* reduces the number of channels to scan, and the *caching* even omits the scanning step based on the previously scanned results. However, without knowledge of the location or direction, these schemes will be incorrect if the MSs move in the opposite direction to the previous movement.

Ramani and Savage introduced the *SyncScan* that locates new APs by periodically performing passive scanning in the surrounding channels [7]. However, the existing APs need to be modified in order to synchronize the transmission timing of their beacon frames, and this is not always guaranteed.

The *Neighbor Graph (NG)-based* schemes [5,15,16] have been proposed in order to only scan the channels of the surrounding APs. The information of the neighboring APs is stored in an NG that is constructed by collecting the scanning results or the history of handoffs. However, these schemes do not restrict the number of neighboring APs to less than six when the APs are densely deployed. This causes MSs to perform another handoff to the APs in another direction or in other floors, which results in frequent handoffs and poor service quality.

The *background scanning* schemes [8,17] have been proposed to periodically perform active scanning even before a handoff is triggered. Since the target APs for a handoff are found in advance, the handoff delay can be minimized

by decoupling the scanning step of the handoff procedure. However, these schemes may cause three different problems. First, the interference of other channels caused by the probe packets increases even when users are not roaming. Second, the TCP/UDP can be affected by the background scanning, which results in throughput degradation. Third, the power consumption of the Wi-Fi chipsets increases due to the periodic scanning.

The *location-based* schemes [18,19] have been proposed to perform scanning selectively based on the location of an MS. The Wi-Fi Positioning System (WPS) is used, and the coordinates of the APs and MS are needed to predict the target APs to handoff to. However, the WPS requires a large amount of scanned data to be processed in advance, which is time consuming.

Wanalertlak et al. proposed the *Behavior-based Mobility Prediction* (BMP) mechanism [6], and it performs a fast handoff without scanning by predicting the next AP for connection based on the mobility patterns of the MSs. For example, user affiliation and time of day are used to enhance the accuracy of the prediction. However, the prediction may be incorrect because VoIP users occasionally roam in random patterns without a definite purpose.

IEEE standards 802.11r [20] and 802.21 [21] are specified to provide some messaging primitives to control a handoff; however, these standards do not specify how the MSs find out new APs and what APs the MSs should handoff to. As the well-known manufacturers of smartphone Wi-Fi chipset, Broadcom, TI, and Qualcomm use both the conventional handoff that scans all channels and a periodic scanning scheme that is similar to the *background scanning* in their Wi-Fi driver [22–24]. However, these two schemes have the disadvantages as mentioned above, and mobile users are still experiencing poor service quality on the move with their smartphones.

2.3. Related work on video delivery

These handoff studies, however, only consider the handoff delay and do not measure and analyze the perceptual quality of real-time video in real environments with frequent handoffs. In addition, these studies do not consider the packet losses that occur at or around the time of handoffs. Although some studies mention the packet loss problem, these studies only consider the packet losses that occur at the time of handoffs. For example, Chou and Shin proposed the *Buffering-and-Forwarding* scheme that forwards the packets buffered at the old AP before a handoff to the new AP [25]. However, this scheme cannot manage the packet losses that occur around the time of handoffs, and it requires modification of the existing APs in order to implement the modified Inter-Access Point Protocol (IAPP).

Ksentini et al. proposed the *Differential Transmission* scheme that uses IEEE 802.11e and transmits video frames according to their priorities in decoding [26]. The scheme increases the probability of successful frame transmission by allotting shorter Inter-Frame Spaces (IFSs) to video frames with higher priority than video frames with lower priority. Consequently, the video quality is enhanced to a

certain degree, but visual quality degradation still occurs due to the packet losses.

Apple Inc. proposed *HTTP Live Streaming* (HLS), which is a well-known protocol for transmitting broadcasts and Video-on-Demand (VoD) [27]. Because HLS is a TCP-based protocol, there is no frame loss or frame distortion in the video. However, HLS is not suitable for delivering real-time video due to its latency (approx. 30 s) [28].

More recently, Dely et al. proposed a *Software-Defined Networking* (SDN)-based scheme for handoff that also considers video delivery [29]. However, video freeze events are only considered due to the usage of an HTTP-based streaming that is not suitable for hard real-time multimedia services, such as video conferencing.

Therefore, a new fast handoff scheme with a transmission method is required in order to both reduce the handoff delay and maintain the quality of real-time video even when packet losses occur. These two issues are equally important for real-time multimedia services and must be considered together in order to support user mobility.

3. Directional Handoff scheme

The proposed DH scheme predicts the direction of an MS using a geomagnetic sensor embedded in the mobile device; this enables the reduction of the handoff delay by only scanning the candidate APs that exist in the predicted direction. This is performed using an *Access Point Table* (AP Table) that stores at most two candidate APs to scan with respect to the locations of the APs and the movement direction of the MS.

3.1. Overall procedure

Fig. 2 presents the flowchart of the proposed DH scheme. First, an MS checks the RSSI of the currently associated AP. Whenever an MS receives a packet, the current RSSI ($RSSI_{Current}$) is calculated using the following formula:

$$RSSI_{Current} = RSSI_{Previous} \times (1 - \lambda) + RSSI_{Measured} \times \lambda, \quad (4)$$

where $RSSI_{Previous}$ is the previous RSSI value calculated using Eq. (4), $RSSI_{Measured}$ is the RSSI value measured from the last received packet, and λ ($0 \leq \lambda \leq 1$) is an RSSI filter weight that determines how much $RSSI_{Measured}$ reflects the current RSSI. In this study, a λ value of 0.4 is used.

If the $RSSI_{Current}$ is less than the handoff threshold, the scanning process is initiated (Step 2 in Fig. 2). Before scanning, the candidate APs to scan and their channels must be chosen. In the proposed DH scheme, an MS selects the candidate APs depending on its movement direction. An MS uses its geomagnetic sensor to obtain its movement direction (Step 3 in Fig. 2; the detailed procedure is described in Section 3.2). Thereafter, the indices of the candidate next APs are retrieved from the AP Table (Step 4 in Fig. 2). These indices are used to retrieve the MAC addresses and channel frequencies from a *Mapping Table* that stores this information for all APs.

Afterwards, the MS performs active scanning only the channels of the candidate APs (Step 5 in Fig. 2). The MS transmits the probe request frames through unicasting

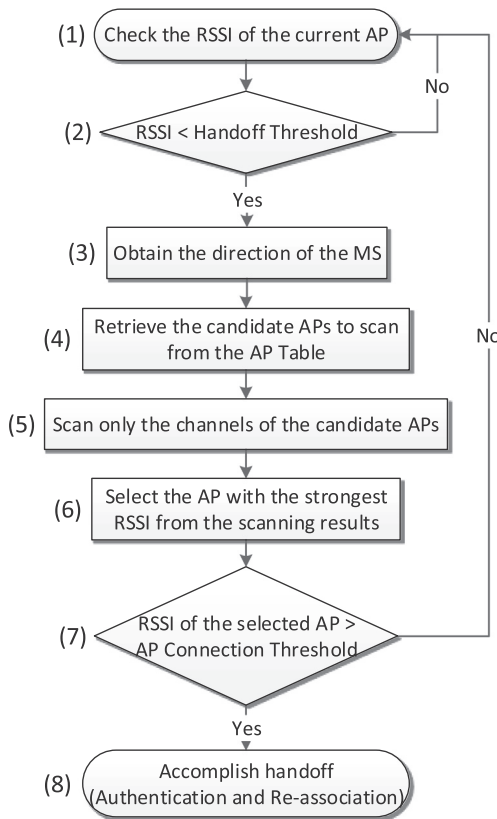


Fig. 2. Flowchart of the Directional Handoff scheme.

based on the MAC addresses and channel frequencies retrieved from the Mapping Table. In this manner, if the MS receives probe response frames before *MinChannelTime*, it does not need to wait for additional probe response frames and can immediately switch to the next channel. However, if there are no candidate APs from the AP Table, the MS performs active scanning on all channels through broadcasting to find all APs and waits until *MaxChannelTime* even when the MS receives a probe response frame before the *MinChannelTime*.

After the scanning step, if there is more than one candidate AP scanned, the AP with the strongest RSSI is selected (Step 6 in Fig. 2). Afterwards, this value is compared with that of the AP connection threshold (Step 7 in Fig. 2). For example, if the threshold is -70 dBm, the MS only connects to the AP whose RSSI is greater than -70 dBm. This minimizes the Ping-Pong effect (i.e., oscillating handoffs) [7]. Finally, the authentication and re-association steps are performed to complete the handoff.

In Steps 1 and 2, we use the current RSSI value as a handoff trigger, although there are other indicators, such as physical transmission rate [8] or bandwidth estimation of APs [30]. However, the RSSI value is still widely used by the Wi-Fi chipset manufacturers and can easily be accessed by user-level software for a cross-layer design. In terms of the λ value, it needs to be generalized because a lot of applications (e.g., WPS) also use the RSSI value, and the Wi-Fi chipset manufacturers use their own fixed λ values that are not optimal.

3.2. Obtaining the movement direction

This section describes the procedure for obtaining the movement direction of an MS (Step 3 in Fig. 2). Current smartphones and pad/tablet devices have a variety of sensors, including an acceleration sensor (accelerometer), a geomagnetic sensor (digital compass or orientation sensor), and so on. The proposed DH scheme uses the geomagnetic sensor to obtain the azimuth of an MS, which is defined as the angle measured clockwise from the magnetic north of the Earth to the y -axis of the MS. The symbol α in Fig. 3 denotes the azimuth of an MS. α varies from 0° to 360° , where 90° is east, 180° is south, 270° is west, and 0° and 360° represent north.

The procedure for obtaining the movement direction of an MS is summarized in the following six steps.

- Step 1. Receive an event from the sensor manager.
- Step 2. Retrieve the azimuth of the MS.
- Step 3. Obtain the screen orientation.
- Step 4. Calibrate the azimuth according to the screen orientation.
- Step 5. Convert the azimuth into one of the compass points.
- Step 6. Calculate the mode from the compass points collected for 5 s.

The azimuth is obtained by receiving an event from the *sensor manager* (Steps 1 and 2), which is a component in a mobile operating system, such as Android OS. The *sensor manager* tracks the changes in the angle using the geomagnetic sensor and provides this information as events to the other components and user-level software. In order to receive these events, the procedure specifies the type of sensor to be tracked and the time interval to the *sensor manager*. In the proposed implementation, a time interval of 50–200 ms is used, which is sufficient to obtain the direction of the MS.

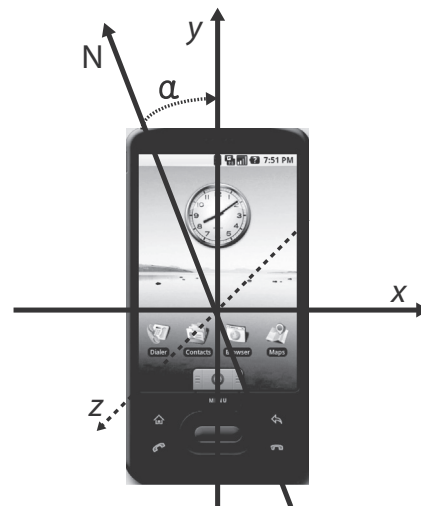


Fig. 3. Three axes of a geomagnetic sensor and the azimuth α .

There are two considerations to be made in using the azimuth. The first consideration is related to the screen orientation (portrait mode vs. landscape mode) of an MS. Fig. 3 illustrates the portrait mode. If the MS is turned sideways, then it becomes the landscape mode. If the screen mode changes from portrait to landscape, the azimuth should be calibrated as follows (Steps 3 and 4):

- If the MS is on its left side, (α_{Left} : before calibration, α : after calibration)

$$\alpha = \begin{cases} \alpha_{Left} + 90^\circ, & \text{if } \alpha_{Left} \leq 270^\circ \\ \alpha_{Left} - 270^\circ, & \text{otherwise} \end{cases} \quad (5)$$

- If the MS is on its right side, (α_{Right} : before calibration, α : after calibration)

$$\alpha = \begin{cases} \alpha_{Right} - 90^\circ, & \text{if } \alpha_{Right} \geq 90^\circ \\ \alpha_{Right} + 270^\circ, & \text{otherwise} \end{cases} \quad (6)$$

The screen orientation (or screen mode) is obtained by invoking Application Programming Interface (API) commands. Because the mobile OS must display its screen differently according to the screen orientation, it also traces the changes in the values of the geomagnetic sensor. Note that the geomagnetic sensor products developed by Asahi [31] and Yamaha [32] consume very little power (typically 1–30 mW), which is lower than the other sensors discussed in [33]. Therefore, the continuous use of the geomagnetic sensor has a minimal impact on the total power consumption.

The second consideration is related to phone calls. When an MS changes to the phone call mode, which is identified from the pitch value (rotation around the x -axis in Fig. 3), the azimuth must be calibrated based on Eqs. (5) or (6) depending on which ear is used. Whether a user is holding the phone to left ear or right ear can be recognized by the help of an accelerometer sensor.

For example, when the pitch value is lower than -50 , the accelerometer sensor is activated. If the x -axis value of the accelerometer is greater than 5, which indicates that the left ear is used, Eq. (5) is used to calibrate. On the other hand, if the x -axis value is lower than -5 , which indicates that the right ear is used, Eq. (6) is used.

After the calibration, the procedure converts the azimuth into one of the eight compass points shown in Table 1 (Step 5). Finally, the procedure calculates the mode from the compass points collected over a period of 5 s (Step 6) because it is not sufficient to use only one compass point due to the sensitivity of the geomagnetic sensor.

Table 1
Conversion between azimuths and compass points.

Azimuth	Direction	Azimuth	Direction
0–22, 338–360	N	158–202	S
23–67	NE	203–247	SW
68–112	E	248–292	W
113–157	SE	293–337	NW

3.3. AP Table structure

The AP Table is a data structure that stores the candidate APs for scanning with respect to the AP locations and the movement direction of the MS. An AP Table can be manually or automatically constructed, and an automatic construction scheme is proposed in Section 3.4. The constructed AP Table is stored in a server (co-located with an authentication server), which is downloaded to the MSs when they first join the network.

Table 2 presents an example AP Table for the network topology shown in Fig. 4, where both MS A and MS B are associated with AP1 and are moving towards AP2. Each row stores the current AP index, direction, and indices of at most two candidate APs to scan in the movement direction. The AP Table contains up to two candidate APs for each direction because, at most, two APs with the same Service Set Identifier (SSID) cover each direction in Fig. 4.

Table 2 only presents the entries whose current AP index is AP1, but the information of other APs is recorded in the same manner. In addition, the table only uses the indices of the APs in order to eliminate redundancy. As mentioned above, the MAC addresses and channel frequencies of the APs are stored in a Mapping Table (not shown), which simplifies the updating process when the APs and/or channel frequencies change.

From the AP Table, an MS can easily determine the candidate APs to scan in advance. For example, MS A in Fig. 4 is moving toward the east and discovers that the candidate AP is AP4 through searching the AP Table. The MS will then perform a handoff to AP4 through only scanning the channel 6 of AP4.

Although the proposed DH scheme does not distinguish the locations of both MSs in Fig. 4, only MS A can handoff to AP4 because when MS B scans channel 6 of AP4, the scanning result will not return AP4 as an available AP. Therefore, the proposed DH scheme prevents MSs from handing off to incorrect APs because the movement direction and scanning result together indicate the approximate location of an MS.

3.4. Automatic AP Table construction

If an AP Table for the network does not exist, the proposed construction scheme automatically builds an AP Table for the network and uploads it to the server. In order to determine the candidate APs for scanning in a direction, the proposed construction scheme uses a geomagnetic

Table 2
AP table for the environment shown in Fig. 4.

Current AP	Direction	Next AP1	Next AP2
AP1	N	AP2	AP3
AP1	NE	AP3	AP4
AP1	E	AP4	–
AP1	SE	AP4	AP5
AP1	S	AP5	AP6
AP1	SW	AP6	AP7
AP1	W	AP7	–
AP1	NW	AP7	AP2

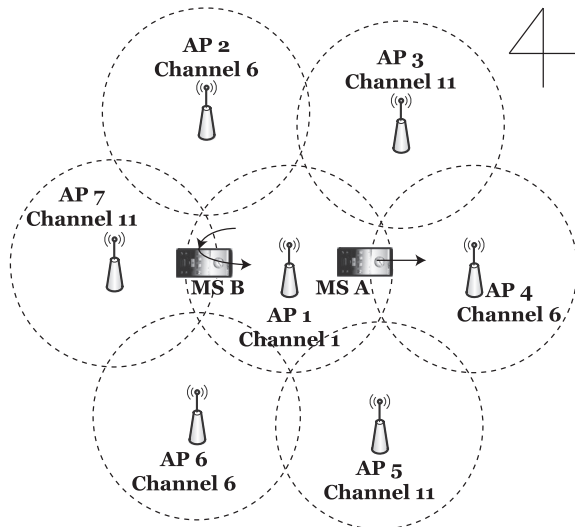


Fig. 4. An example of WLAN deployment in an environment without obstacles (MSs A and B are associated with AP1).

sensor and accumulates the scanning results with respect to the direction of an MS.

In order to simplify the proposed algorithm, a common handoff scenario is modeled as shown in Fig. 5, where the MS is associated with AP1 and is moving towards AP2. A user in the scenario can walk, run, or stop for a while only if the MS maintains its movement direction within a valid range, e.g., *initial azimuth direction* $\pm 90^\circ$. We assume that the user is moving along the shortest path; reversing the direction is not allowed.

In addition, a threshold, called the *Construction Threshold*, is defined in order to restrict the area where the proposed algorithm operates by assigning a value greater than both the handoff threshold and AP connection threshold. Therefore, the proposed algorithm begins before the handoff process and finishes after the handoff, which ensures that the MS is moving from one AP to another and is moving closer to one of the candidate APs.

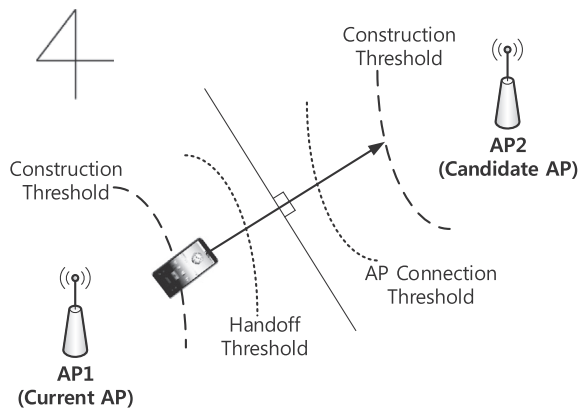


Fig. 5. A common handoff scenario and construction threshold.

Fig. 6 presents the flowchart for the proposed construction scheme derived from the modeling. First, if the RSSI of the current AP is lower than the construction threshold, active scanning is performed every two seconds (Steps 1–3). This scanning interval produces a sufficient amount of scanning data and is recommended for scanning in order to co-exist with TCP and UDP applications [34].

Next, the scanning result is stored with both the movement direction of the MS and the RSSI of the AP that the MS is initially associated with (Step 3). Afterwards, the scheme verifies whether or not the movement direction is in the valid range of movement (Step 4). If the user is moving in the opposite direction, then the scheme stops and discards the scanning results collected thus far (Step 5).

After a handoff, when the RSSI of the connected AP becomes greater than the construction threshold, the average RSSI after the handoff is calculated with respect to each AP (Steps 6 and 7). Finally, the AP whose average RSSI is the lowest is stored in the AP Table with two directions that are recorded after the handoff threshold (Step 8). In addition, the average RSSI is also stored for the server to perform crowdsourcing on the data gathered from many devices.

Our construction scheme does not require WPS or the use of other sensors in order to determine the distance between APs. In addition, the experimental results in real WLAN environments, which are described in the next section, demonstrate that the proposed scheme accurately constructs an AP Table even if the RSSI fluctuates. The lower bound on the accuracy of the construction scheme is 90%.

4. Implementation of the directional handoff with VoIP analysis

In this study, the following mobile devices are used in this study:

- Motorola Defy: 800 MHz single-core CPU, 512 MB RAM, Texas Instruments WL1273 Wi-Fi chipset, which supports only 2.4 GHz band.
- LG Optimus LTE2: 1.5 GHz dual-core CPU, 2 GB RAM, Qualcomm Atheros Wi-Fi chipset, which supports 2.4 and 5 GHz bands.

The devices are Android platform-based smartphones. Android is open source software [35] and the Wi-Fi driver source codes for the devices are also open source [23]. Note that the proposed DH scheme does not require modification to the existing APs.

4.1. Cross-layer implementation

The DH scheme uses a cross-layer implementation as shown in Fig. 7. The user-level application provides the candidate AP information to the Wi-Fi driver through Socket Inter-process Communication (IPC). In addition, the application downloads an AP Table from the server through a TCP connection if the table exists in the server; otherwise, the application automatically constructs an AP Table and uploads it to the server. Moreover, the

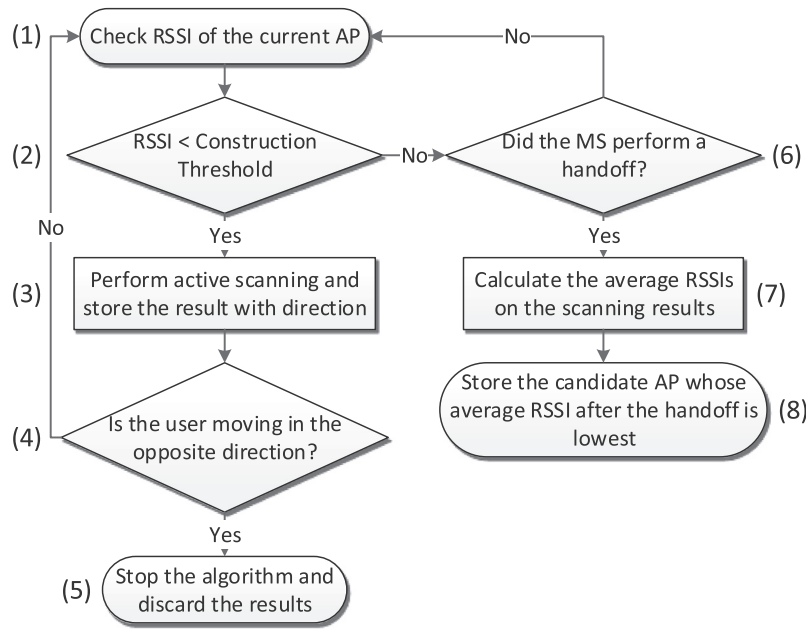


Fig. 6. Flowchart for the AP Table construction scheme.

application generates or receives Constant Bit Rate (CBR) traffic for evaluation assuming a VoIP application.

The Wi-Fi driver scans and then selects the target AP to reconnect with and conducts a handoff. In addition, it logs the time when a UDP packet is transmitted or received through the wireless medium. In this way, our cross-layer design can be implemented without modifying Android OS.

4.2. Experimental environment

The proposed DH scheme was tested on the following three WLAN environments at KAIST:

- The 1st and 2nd floors of the CS building (Fig. 8(a)): The floor size is $120 \times 70 \text{ m}^2$, and each floor has 6 APs. The distance between the APs is around 20 m, and there are a few obstacles (e.g., walls) between the APs. The network uses 2.4 GHz band and Open authentication.
- The 1st floor of the KI building (Fig. 8(b)): The floor size is $100 \times 120 \text{ m}^2$ and has two APs. This environment is an open space, and the distance between the APs is around 40 m. The network uses 5 GHz band and 802.1X authentication.
- The 7th and 8th floors of the N1 building (Fig. 8(c)): The floor size is $70 \times 30 \text{ m}^2$, and each floor has 8 APs. The distance between the APs is around 17 m, and there are many obstacles between the APs. The network uses 5 GHz band and 802.1X authentication.

All APs in each environment have the same SSID; therefore, only the link layer handoff is considered. In addition, these APs are installed for general purpose and are used by a lot of students, staffs, and faculty members, which indicates that there is much background traffic in daytime.

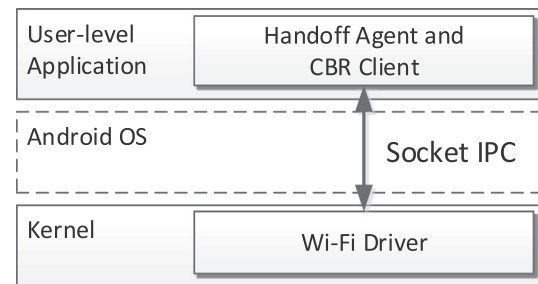


Fig. 7. Cross-layer implementation.

The performance evaluation is based on a bidirectional data transmission between smartphone and PC. Because the Motorola Defy only supports 2.4 GHz band, we use it in the CS building, and we use LG Optimus LTE2 in the other buildings. The PC is located in a building next to the CS building and uses the Windows 7 operating system. The smartphone and PC generate CBR traffic for a VoIP application, and the size of the data packet generated is 200 bytes including the IP and UDP headers (transfer rate: 50 packets/s = 80 Kbps).

The handoff-related parameters and their values used in the experiments are summarized in Table 3. The proposed DH scheme was compared with the Conventional Handoff (CH) scheme that performs scanning on all channels and the Selective Scanning (SS) scheme used in [4]. The caching mechanism in [4] was not used because it causes MSs to connect to incorrect APs in the opposite direction to their movement, which leads to frequent disruptions. In addition, the evaluation of the SS scheme in the 5 GHz band was excluded because the scheme basically includes the orthogonal channels and there are a lot

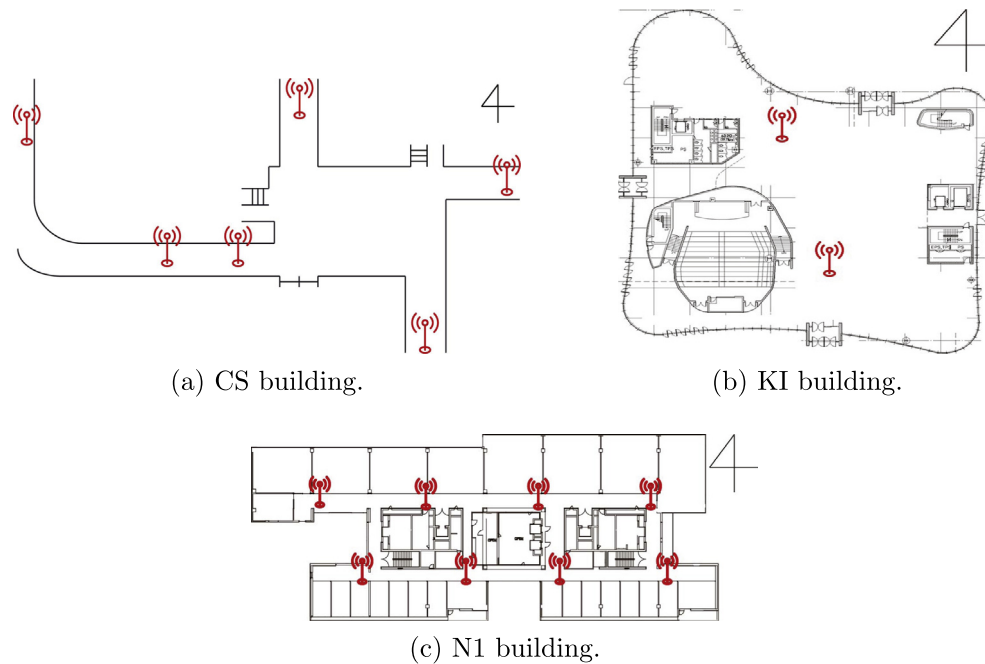


Fig. 8. Enterprise WLAN environments of the three buildings at KAIST.

of orthogonal channels in the 5 GHz band. Finally, all the schemes use active scanning on non-DFS channels and passive scanning on DFS channels as mentioned in Section 2.

4.3. Experimental results for VoIP

For evaluation, we randomly walked in each of the three WLAN environments as shown in Fig. 8, and gathered more than 70 handoff samples for each scheme in each WLAN environment. When performing the experiments, we assumed that a user is watching the mobile device and occasionally changes the portrait mode of the MS to the landscape mode, and vice versa. In addition, before we evaluated the DH scheme, we walked all available paths in each WLAN environment more than two times, in order to construct an AP Table. All the experiments were performed in daytime from 10 a.m. to 7 p.m. when a lot of users are using the networks.

As a result of the experiments, Fig. 9 presents the distribution of scanning delays and the distributions of number of packet losses that occurred for three seconds before each handoff. First, as shown in Fig. 9(a), the DH scheme greatly reduces the scanning delay in the 5 GHz band (KI and N1 buildings) since it only scans one or two channels among total 19 channels.

When we compare the results of the DH scheme in the KI and N1 buildings, the scanning delay in the KI building is lower than that in the N1 building since the first floor of the KI building only has two APs, thereby producing only one candidate AP during scanning. In addition, 10% of the scanning delays in the N1 building are resulted from full scanning, compared with 3.9% in the KI building. This is because the DH scheme in the N1 building occasionally

fails to find out the target AP more than that in the KI building, which results in more full scanning. Compared to the open space in the KI building, the DH scheme in the N1 building has higher probability of scanning failure due to the misprediction of the movement direction, abrupt errors in the geomagnetic sensor, and incorrect AP Table entries.

In the 2.4 GHz band (CS building), the DH scheme also reduces the scanning delay compared with the SS and CH schemes. The SS scheme performs full scanning frequently (41.5%) because the channel mask in the SS scheme [4] is inverted whenever the scheme fails to find out the target AP to handoff to.

In terms of the number of packet losses at client-side, as shown in Fig. 9(b), the DH scheme reduces the number of packet losses by half in the 5 GHz band. In the 2.4 GHz band, the DH scheme also reduces the number of packet losses compared with the SS and CH schemes although the improvement is not high. After analyzing the causes of the packet losses, we found that the scanning step in the handoff process causes most packet losses, and the scanning delay affects the number of packet losses.

Because the MS cannot receive packets from the current AP while scanning, a notification frame is sent to the current AP to buffer the incoming packets during scanning. However, this notification frame can also be lost, which in turn cannot avoid packet losses during scanning. Therefore, the objective of the proposed approach is to reduce the scanning delay as much as possible.

On the other hand, the number of packet losses at server-side is not affected by the scanning delay, as shown in Fig. 9(c), because the MS does not transmit data packets during scanning. Instead, deciding the appropriate target

Table 3
Handoff-related parameters and their values.

	CH	SS	DH
Scanning method	Scanning on all channels	Scanning selectively	
Handoff threshold	-76 dBm		
MinChannelTime	6.5 ms		
MaxChannelTime	11 ms		
Probe request trans.	Broadcasting		Unicasting
Early termination	Off		On
AP connection threshold	-70 dBm		
Periodic passive scanning	Off		
RSSI filter weight	0.4		

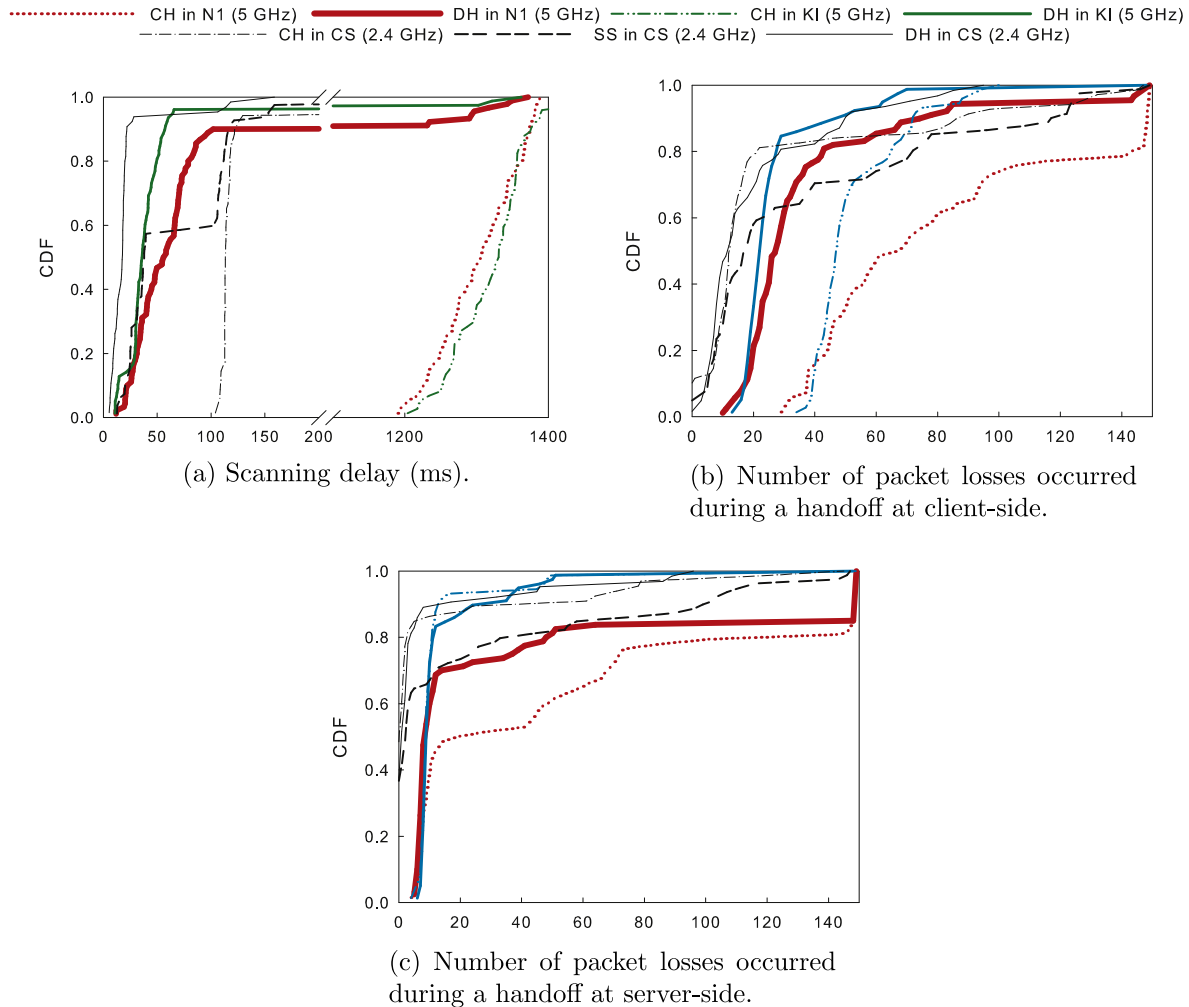


Fig. 9. Analysis of CBR traffic.

AP to handoff to is more important when we compare the results of the DH and CH schemes in the N1 building where the APs are densely deployed. The CH scheme in the N1 building occasionally performs handoffs to the APs in other floors, which results in increased noise levels at the APs.

Table 4 summarizes the average delays and the average number of packet losses with their standard deviations. The authentication and re-association delays are not

shown in the table because both delays are within 5 ms and thus have minimal impact on the handoff delay.

The above explanation for Fig. 9 is also applied to this table. Furthermore, we found that today's Wi-Fi drivers uncouple each step of the handoff process, which results in higher handoff delay. However, as shown in Fig. 1, data packets can be transmitted between each step; therefore, the inter-packet arrival time is maintained if there are no

packet losses. This kind of uncoupling is essential for the Wi-Fi drivers since they have already become complex systems in order to implement a lot of features including authentication, encryption, handoff, power management, and so on.

5. Delivery of real-time video with directional handoff using Lightweight Retransmission Protocol (LRP)

This section discusses the proposed LRP, which is a real-time video transmission protocol, over WLANs for mobile users, and it operates in the *Transport* layer as an end-to-end protocol. The LRP minimizes the number of lost video packets using retransmissions and ensures timely play-out of video packets using timers.

5.1. Lightweight Retransmission Protocol (LRP)

Fig. 10 presents the LRP stack, which relies on the Real-time Transport Protocol (RTP). The LRP that runs on the server side identifies whether or not a packet generated in the *Application* layer is a video packet by examining the *Payload Type* field of the RTP header. If a packet contains video information, then it is stored in a buffer, called the LRP buffer, before being sent to the *Network* layer through the UDP. The LRP buffer functions as a retransmission buffer in order to allow the lost packets to be resent.

Fig. 11 illustrates an example message flow between an LRP server and client. In the LRP, there are three types of timeouts: $Timeout_R$, $Timeout_D$, and $Timeout_A$. Both $Timeout_R$ and $Timeout_D$ are associated with each packet, whereas $Timeout_A$ is associated with a group of packets. The LRP on the server side transmits a packet and then waits $Timeout_R$ for a corresponding LRP acknowledgement (ACK) packet from the client. If the corresponding ACK arrives before $Timeout_R$ expires, the server deletes the packet from the LRP buffer; otherwise, the packet is retransmitted.

The LRP uses a selective acknowledgement scheme, where the client transmits a single ACK to the server after receiving one or more LRP packets within $Timeout_A$. This significantly improves the performance and efficiency of WLANs compared with sending an individual ACK for each received packet.

The server deletes the packets that are not acknowledged within $Timeout_D$ that is greater than both $Timeout_R$

and $Timeout_A$. Therefore, the LRP does not guarantee reliable transmission for all packets.

5.1.1. Implementation details

The LRP buffer consists of a doubly linked list as shown in Fig. 12. Each buffer entry represents one LRP packet and stores not only packet data but also various information including a sequence number, a timestamp, and size. The *Sequence Number* field stores the sequence number extracted from the RTP header. The *Timestamp* field stores the time in microseconds when the packet was forwarded to the *Network* layer (in the server) or forwarded from the *Network* layer (in the client), and it is used to operate timers.

The server-side LRP does not add a separate header to packets delivered from the *Application* layer. Instead, the *Protocol Identifier* field of the IP header is modified. The protocol number of 253 is assigned to the field, which is originally reserved for experimental use.

After an LRP packet is forwarded to the *Network* layer, $Timeout_R$ and $Timeout_D$ are initiated for the forwarded packet. In this study, $Timeout_R$ is set to 140 ms, which is determined considering the end-to-end delay that is preferred for most user applications (0–150 ms) recommended by ITU [11]. In addition, $Timeout_D$ is set to 400 ms, which is the maximum allowed end-to-end delay for real-time multimedia [11]. While this study uses a fixed value for simplicity, adaptively adjusting $Timeout_R$ according to the network conditions could lead to better results. This remains as future work.

The client-side LRP sends an ACK after receiving some packets from the server. The structure of the LRP ACK is shown in Fig. 13. An LRP ACK is appended to the end of the IP header and has a variable number of *Sequence Number* fields. The *Num* field is 2-byte long and indicates the number of *Sequence Number* fields to be acknowledged within $Timeout_A$ (50 ms in this study).

The client-side LRP also tracks the sequence numbers of the received packets. When the packets arrive in order, the LRP sends them directly to the upper layer without storing them in the LRP buffer. When an out-of-order packet arrives (e.g. in packet loss or out-of-order delivery), the LRP stores the packet in the buffer without sending it to the upper layer. When the packet is stored, the LRP maintains the order of packets in the buffer in an increasing order of sequence numbers. The detailed behavior of the client-side LRP is given in the following code.

Table 4

The average delays and the average number of packet losses with their standard deviations (in parenthesis).

	CH in N1	DH in N1	CH in KI	DH in KI	CH in CS	SS in CS	DH in CS
Scanning delay (ms)	1303 (55.1)	176.9 (378.2)	1327 (76.2)	85.9 (250.5)	135.0 (84.3)	74.6 (79.2)	22.0 (27.4)
Handoff delay (ms)	1537 (267.5)	409.8 (474.6)	1499 (178.8)	242.0 (249.8)	322.1 (758.1)	128.4 (111.7)	63.9 (31.4)
Num. of packet losses at client-side	80.6 (41.7)	38.4 (31.4)	52.8 (14.7)	27.9 (18.7)	27.2 (37.7)	38.6 (41.6)	21.0 (21.7)
Num. of packet losses at server-side	52.6 (54.6)	35.7 (51.7)	13.4 (18.4)	14.6 (18.2)	10.9 (28.6)	23.2 (40.6)	7.9 (20.5)

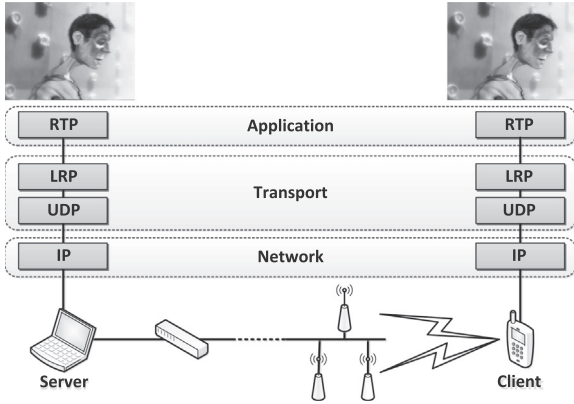


Fig. 10. Lightweight Retransmission Protocol (LRP) stack.

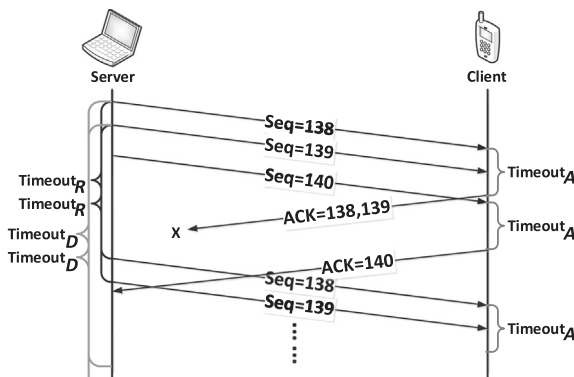


Fig. 11. An example of an LRP message flow.

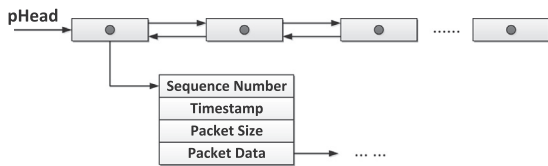


Fig. 12. LRP buffer structure.

```

N; {Sequence number of the received LRP packet}
SEQ; {Last sequence number received in order}
if  $N < (SEQ + 1)$  then
    Discard the packet;
else if  $N > (SEQ + 1)$  then
    Store the packet in the LRP buffer;
else if  $N = (SEQ + 1)$  then
    Forward the packet to the upper layer;
    if The LRP buffer is empty then
         $SEQ \leftarrow (SEQ + 1)$ ;
    else
        Forward the consecutive packets that start
        with  $(N + 1)$  in the buffer;
        Delete the forwarded packets in the buffer;
        Update SEQ based on the number of packets
        forwarded;
    end if
end if
    
```

For example, suppose SEQ is 99 and the buffer contains packets with the sequence numbers 101–103 and 105–107. If a packet with the sequence number 100 arrives, then the arriving packet and the packets of 101–103 in the buffer are forwarded to the upper layer, and SEQ is updated to 104.

Finally, the client-side LRP also has a timer to delete old packets stored in the buffer. The timer is used to delete the packets that have been stored for $Timeout_D$, and these packets are also forwarded to the upper layer to be decoded and played.

5.2. Experiments and analysis

For evaluation, a lot of experiments were conducted based on the same environments as discussed in Section 4.2. The test video used was *Big Buck Bunny* [36] with a duration of 9 min 54 s. We randomly walked in each of the WLAN environments until the test video finished playing, and we gathered the data corresponding to more than 2 h for each scheme in each WLAN environment A real-time video server (PC) that is located in a building next to the CS building streamed the video to the smartphone: Motorola Defy or LG Optimus LTE2. The applications and encoding options that were used are described below:

- Applications: The video server uses *VLC Media Player* [37], and the smartphone uses the *MX Player* [38] Android application.
- Encoding options: The specified codec is H.264/AVC with a *Baseline Profile* [40], which is suitable for mobile applications and real-time video. The video is encoded at a frame rate of 24 frames per second with a bit rate of 819 Kbps, and the resolution is 960 (W) \times 540 (H).

The performance comparison was performed using the following protocols: RTP, LRP, and HTTP Live Streaming (HLS). HLS was selected because it is widely used protocol for streaming. Each experiment was conducted using either the Conventional Handoff (CH) scheme or the proposed DH scheme. The selective scanning scheme [4] is not used because its performance is between the CH and DH schemes.

In order to measure the received video quality, the number of frame losses and Peak Signal-to-Noise Ratio (PSNR) were used as metrics. In order to correctly calculate the PSNR, the N th frame of the original video must also be the N th frame in the received video. However, the packet loss in WLANs often leads to frame loss, which causes incorrect PSNR calculation.

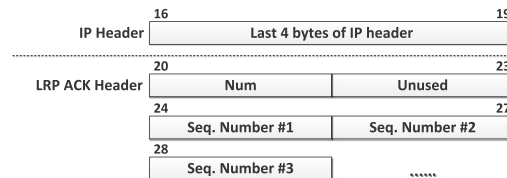


Fig. 13. LRP ACK structure.

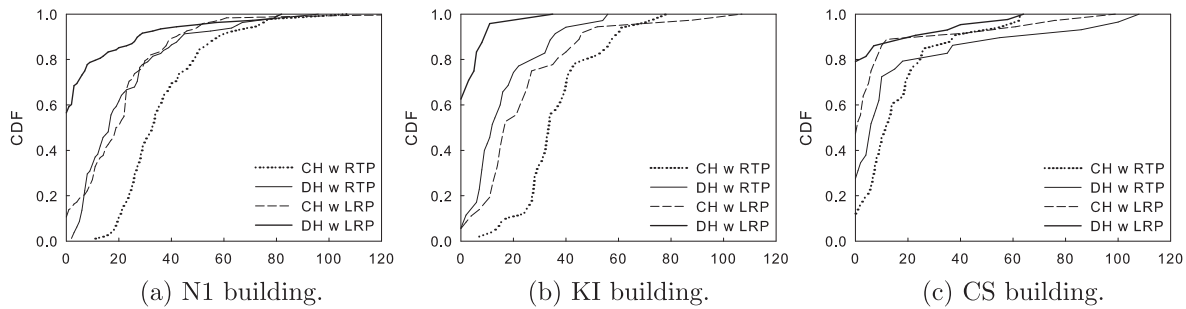


Fig. 14. Analysis of the number of frame losses occurred during a handoff in each WLAN environment.

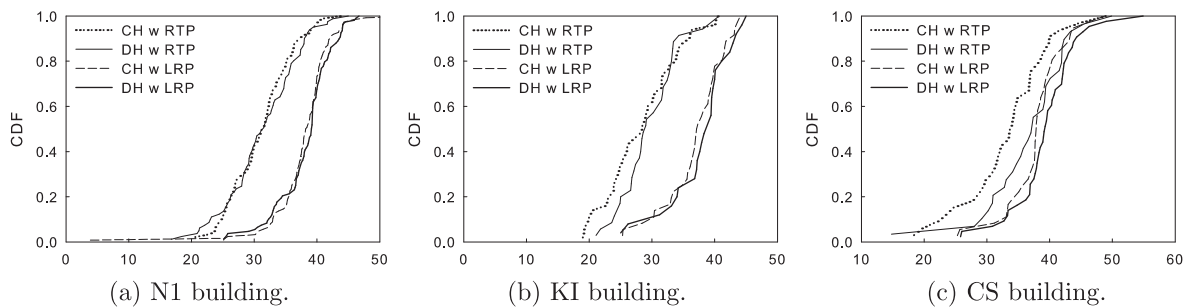


Fig. 15. Analysis of the average values of PSNR (in dB) during a handoff in each of the WLAN environment.

Table 5

Summary of averaged aggregate results with their standard deviations (in parenthesis).

	CH with RTP	DH with RTP	CH with LRP	DH with LRP
N1 building				
Averaged num. of frame losses during a Handoff	37.3 (17.3)	22.2 (19.4)	21.6 (19.5)	8.6 (17.7)
Averaged aggregate PSNR during a Handoff	31.1 (4.9)	31.4 (5.8)	38.2 (3.9)	38.2 (4.4)
KI building				
Averaged num. of frame losses during a Handoff	37.3 (15.2)	16.9 (14.1)	25.0 (22.2)	3.6 (7.4)
Averaged aggregate PSNR during a Handoff	28.3 (5.8)	29.8 (4.7)	37.0 (4.7)	37.8 (5.0)
CS building				
Averaged num. of frame losses during a Handoff	17.1 (16.7)	14.7 (25.2)	10.0 (22.8)	6.1 (15.3)
Averaged aggregate PSNR during a Handoff	33.3 (6.8)	36.7 (6.6)	37.8 (4.7)	39.3 (5.3)

Therefore, an application was developed to perform the frame matching and frame copy. For each frame of the received video, the application locates the corresponding frame in the original video. If a frame is found, it is written to the result video; otherwise, it indicates frame distortion or frame loss, and the frame copy is performed by writing the previous frame to the result video.

Finally, the PSNR values were obtained using the *MSU Video Quality Measurement Tool* [39]. The PSNR values calculated by this application range 0–100 dB, and a PSNR value greater than 31 dB is considered to be good quality. This implies that there is some degradation in perceptual quality but that is not annoying to users.

5.2.1. Experimental results on perceptual quality

Fig. 14 presents the distribution of the number of frame losses that occurred for 6 s during each handoff: three seconds before a handoff and three seconds after the handoff, because packet loss may affect several subsequent frames. In the three environments, the DH scheme with the LRP achieves the lowest number of frame losses, which reduces the duration of video freezing. In addition, in the N1 and KI buildings, the DH scheme with the RTP achieves the second lowest number of frame losses compared with the CH scheme with the LRP. Therefore, the video freezing and the quality degradation due to frame losses can be minimized if the DH scheme and the LRP are simultaneously used.

In the CS building, the CH scheme with the LRP achieves the second lowest number of frame losses compared with the DH scheme with the RTP. Because the scanning delay of the CH scheme in the 2.4 GHz band is lower than $Timeout_D$, the LRP can retransmit a lot of lost packets.

Fig. 15 presents the distribution of the average PSNR value that is calculated for 6 s during each handoff. When the RTP with any handoff scheme is used in the N1 and KI buildings, around 50% of the average values are below 31 dB, which indicates that a user notices the existence of handoffs. On the other hand, when the LRP with any handoff scheme is used in the three environments, at least 86% of the average values are greater than 31 dB, which highly reduces the chance of users' noticing.

In the PSNR results, there are little differences between the handoff schemes because the PSNR is not sufficient to demonstrate the frame loss effects. In addition, since our frame matching and frame copy application operates on the basis of the received video, lost frames are omitted in the PSNR calculation. Therefore, the PSNR results should be considered in conjunction with the number of frame losses.

Table 5 summarizes the results of Figs. 14 and 15. The above explanation for the figures is also applied to this table. In the DH scheme with the RTP or LRP, the number of frame losses is greatly reduced, but this is not reflected in the PSNR.

Finally, we also tested the HLS, but it only succeeds in the 2.4 GHz band (CS building) without service disruption. In the CS building, the HLS with any handoff scheme achieves no frame loss and the highest PSNR due to the nature of TCP. However, in the 5 GHz band (N1 and KI buildings), the HLS is frequently disconnected; we cannot play the test video until the last scene. We found that the MS transmits a TCP RST/FIN message to the web server and closes the connection when a handoff occurs. Therefore, the HLS cannot endure such large number of packet losses and large handoff delay in the 5 GHz band.

6. Conclusion and future work

The DH scheme proposed in this paper performs fast handoffs by scanning a limited number of channels in the 2.4 GHz or 5 GHz bands. This is achieved by predicting the movement direction of an MS using the geomagnetic sensor embedded in the mobile device. The candidate APs to scan are retrieved from the AP Table and active scanning is performed on the channels of the candidate APs. In this paper, the AP Table is constructed automatically when a user first enters a building and no AP Table is found in the server. The Lightweight Retransmission Protocol (LRP) for mobile users is also proposed, which enhances the video quality in packet loss-prone environments, such as handoff areas and areas with severe interference, by retransmitting lost packets.

The experiments using commercial smartphones demonstrate that the scanning and handoff delays are greatly reduced. The proposed DH scheme reduces 90% of the scanning delays to below 150 ms, which allows real-time multimedia services, such as VoIP, to be supported. In addition, the proposed prediction of the movement direction

achieves the accuracy of 90% even in the environment where there are a lot of obstacles between APs. The experiments on the DH scheme with the LRP demonstrate that the quality of real-time video can be maintained consistently, even while users are roaming. The proposed DH scheme with the LRP can be applied to IEEE 802.11b/g/n/ac standards and is compatible with the existing WLANs because it does not require modification to the existing APs. For future work, fast handoff in an outdoor WLAN environment will be investigated.

Acknowledgments

This work was supported in part by the National Research Foundation (NRF) of Korea Grant funded by the Korea Government (MEST) (No. 2012R1A2A2A01008244). A preliminary version of this work [1] was presented at IEEE PerCom 2012, Lugano, Switzerland.

References

- [1] S. Han, M. Kim, B. Lee, S. Kang, Directional Handoff using geomagnetic sensor in indoor WLANs, in: IEEE International Conference on Pervasive Computing and Communications, PerCom, March 2012, pp. 128–134.
- [2] E. Kaplan, C. Hegarty, *Understanding GPS: Principles and Applications*, second ed., Artech House, Boston, 2006.
- [3] P. Bahl, V.N. Padmanabhan, RADAR: an in-building RF-based user location and tracking system, in: IEEE INFOCOM, 19th Annual Joint Conference of the IEEE Computer and Communications Societies, 2000, pp. 775–784.
- [4] S. Shin, A.G. Forte, A.S. Rawat, H. Schulzrinne, Reducing MAC layer handoff latency in IEEE 802.11 wireless LANs, in: The Second International Workshop on Mobility Management & Wireless Access Protocols, MobiWac, October 2004, pp. 19–26.
- [5] M. Shin, A. Mishra, W. Arbaugh, Improving the latency of 802.11 hand-offs using neighbor graphs, in: The 2nd International Conference on Mobile Systems, Applications, and Services, MobiSys, 2004, pp. 70–83.
- [6] W. Wanaertlak, B. Lee, C. Yu, M. Kim, S. Park, W. Kim, Behavior-based mobility prediction for seamless handoffs in mobile wireless networks, *Wirel. Netw.* 17 (3) (2011) 645–658.
- [7] I. Ramani, S. Savage, SyncScan: practical fast handoff for 802.11 infrastructure networks, in: IEEE INFOCOM, 24th Annual Joint Conference of the IEEE Computer and Communications Societies, March 2005, pp. 675–684.
- [8] H. Wu, K. Tan, Y. Zhang, Q. Zhang, Proactive scan: fast handoff with smart triggers for 802.11 wireless LAN, in: IEEE INFOCOM, 26th Annual Joint Conference of the IEEE Computer and Communications Societies, May 2007, pp. 749–757.
- [9] A. Mishra, M. Shin, W. Arbaugh, An empirical analysis of the IEEE 802.11 MAC layer handoff process, *ACM SIGCOMM Comput. Commun. Rev.* 2 (33) (2003) 93–102.
- [10] IEEE Std 802.11 for Information Technology-Telecommunications and Information Exchange Between Systems-Local and Metropolitan Area Networks-Specific Requirements, Part 11: Wireless LAN Medium Access Control (MAC) and Physical Layer (PHY) Specifications, June 2007.
- [11] International Telecommunication Union, End-user multimedia QoS categories, ITU-T G.1010, 2001.
- [12] List of WLAN channels – Wikipedia. <http://en.wikipedia.org/wiki/List_of_WLAN_channels>.
- [13] Dynamic Frequency Selection – Cisco. <<http://www.cisco.com/c/en/us/td/docs/routers/access/3200/software/wireless/3200WirelessConfigGuide/RadioChannelDFS.pdf>>.
- [14] D.J. Leith, D. Malone, Field measurements of 802.11 collision, noise and hidden-node loss rates, in: The 8th International Symposium on Modeling and Optimization in Mobile, Ad Hoc and Wireless Networks, WiOpt, 2010, pp. 412–417.
- [15] S. Park, H. Kim, C. Park, J. Kim, S. Ko, Selective channel scanning for fast handoff in wireless LAN using neighbor graph, *Personal Wirel. Commun.* 3260 (2004) 194–203.

- [16] P.J. Huang, Y.C. Tseng, K.C. Tsai, A fast handoff mechanism for IEEE 802.11 and IAPP networks, in: IEEE Vehicular Technology Conference, VTC, vol. 2, May 2006, pp. 966–970.
- [17] N. Mustafa, W. Mahmood, A.A. Chaudhry, M. Ibrahim, Pre-scanning and dynamic caching for fast handoff at MAC layer in IEEE 802.11 wireless LANs, in: Proceedings of IEEE International Conference on Mobile Adhoc and Sensor Systems Conference, MASS, November 2005, pp. 122–129.
- [18] C.C. Tseng, K.H. Chi, M.D. Hsieh, H.H. Chang, Location-based fast handoff for 802.11 networks, IEEE Commun. Lett. 9 (4) (2005) 304–306
- [19] I. Purushothaman, S. Roy, FastScan: a handoff scheme for voice over IEEE 802.11 WLANs, Wirel. Netw. 16 (7) (2010) 2049–2063.
- [20] IEEE Std 802.11r, Amendment to IEEE Std 802.11–2007, Part 11: Wireless LAN Medium Access Control (MAC) and Physical Layer (PHY) Specifications, Amendment 2: Fast Basic Service Set (BSS) Transition, 2008.
- [21] IEEE Std 802.21, IEEE Standard for Local and Metropolitan Area Networks Part 21: Media Independent Handover Services, 2009.
- [22] Source Code for Broadcom Wi-Fi Chipsets. <<https://android.googlesource.com/platform/hardware/broadcom/wlan/>>.
- [23] Source Code for TI Wi-Fi Chipsets. <<https://android.googlesource.com/platform/hardware/ti/wlan/>>.
- [24] Source Code for Qualcomm Chipsets. <<https://android.googlesource.com/kernel/msm/>>.
- [25] C.T. Chou, K.G. Shin, An enhanced inter-access point protocol for uniform intra and intersubnet handoffs, IEEE Trans. Mobile Comput. 4 (4) (2005) 321–334.
- [26] A. Ksentini, M. Naimi, A. Gueroui, Toward an improvement of H.264 video transmission over IEEE 802.11e through a cross-layer architecture, IEEE Commun. Mag. 44 (1) (2006) 107–114.
- [27] HTTP Live Streaming – Wikipedia. <http://en.wikipedia.org/wiki/HTTP_Live_Streaming>.
- [28] HTTP Live Streaming Overview – Apple Developer. <<https://developer.apple.com/streaming/>>.
- [29] P. Dely, A. Kassler, L. Chow, N. Bambos, N. Bayer, H. Einsiedler, M. Sanchez, A software-defined networking approach for handover management with real-time video in WLANs, J. Modern Transport. 21 (1) (2013) 58–65.
- [30] P. Dely, A. Kassler, L. Chow, N. Bambos, N. Bayer, H. Einsiedler, C. Peylo, BEST-AP: non-intrusive estimation of available bandwidth and its application for dynamic access point selection, Comput. Commun. 39 (15) (2014) 78–91.
- [31] Asahi KASEI Electronic Compass – AK8973N/B/S, AK8975/B. <<http://www.asahi-kasei.co.jp/akm/en/product/compass.html>>.
- [32] Yamaha Geomagnetic Sensors. <http://www.yamaha.co.jp/english/product/lsi/magnetic_sensor/>.
- [33] Y. Wang, J. Lin, M. Annavaram, Q.A. Jacobson, J. Hong, B. Krishnamachari, N. Sadeh, A framework of energy efficient mobile sensing for automatic user state recognition, in: The 7th International Conference on Mobile Systems, Applications, and Services, MobiSys, 2009, pp. 179–192.
- [34] T. King, T. Haenselmann, S. Kopf, W. Effelsberg, A measurement study on 802.11 concurrently used for positioning and communications, in: The 3rd International Symposium on Wireless Pervasive Computing, ISWPC, May 2008, pp. 610–615.
- [35] Android Open Source. <<http://source.android.com>>.
- [36] Xiph.org Test Media. <<http://media.xiph.org>>.
- [37] VideoLAN – VLC Media Player. <<http://www.videolan.org/vlc/>>.
- [38] MX Player. <<https://sites.google.com/site/mxvpen/>>.
- [39] MSU Video Quality Measurement Tool. <http://compression.ru/video/quality_measure/video_measurement_tool_en.html>.
- [40] T. Wiegand, G.J. Sullivan, G. Bjntegaard, A. Luthra, Overview of the H.264/AVC video coding standard, IEEE Trans. Circ. Syst. Video Technol. 13 (7) (2003) 560–576.



Sangyup Han received his B.A. in Computer Engineering from Kyungpook National University in 2010, and his M.S. in Computer Science from the Korea Advanced Institute of Science and Technology (KAIST) in 2011. He is currently a Ph.D student in Computer Science at the KAIST. His research interests include mobility support in IEEE 802.11, multimedia streaming in wireless and mobile Internet, and wireless MAC protocol.



Myungchul Kim received his B.A. in Electronics Engineering from Ajou University, Korea, in 1982, his M.S. in Computer Science from KAIST in 1984, and his Ph.D. in Computer Science from the University of British Columbia, Canada, in 1993. Currently, he is with the faculty of KAIST as a professor. His research interests include Internet, mobile Internet, protocol engineering, mobile computing, and wireless mesh networks.



Ben Lee received his B.E. degree in 1984 from the State University of New York at Stony Brook, and his Ph.D. degree in Computer Engineering in 1991 from Pennsylvania State University. He is currently with the School of Electrical Engineering and Computer Science at Oregon State University. He has published over 80 conference proceedings, book chapters, and journal articles in the areas of embedded systems, computer architecture, multithreading and thread-level speculation, and wireless networks.



Sungwon Kang received his B.A. from Seoul National University, Korea, in 1982 and received his M.S. and Ph.D. in Computer Science from the University of Iowa, USA, in 1989 and 1992, respectively. From 1993, he was a principal researcher of Korea Telecom R & D Group until October 2001 when he joined KAIST and is currently an associate professor of the university. Since 2003, he has been an adjunct faculty member of Carnegie-Mellon University, USA, for the Master of Software Engineering Program. His current research areas include software architecture, software product line, software modeling and analysis, and software testing.